Controlled Load Tests on a Four-Girder Steel Bridge

J. HAROLD DEATHERAGE, MICHAEL DAVID SANDERS, DAVID W. GOODPASTURE, AND EDWIN G. BURDETTE

A fatigue investigation of the I-40 bridge over the Holston River provided an excellent opportunity to measure and analyze the response of an actual structure to applied loads. During the course of the project, responses to both actual traffic loadings and controlled loadings were measured. In this paper the data collected during the controlled load tests are examined and the means by which the data were collected are outlined. Methods currently used to distribute applied loads to the main structural members have been found to produce conservative results in several cases. This project made it possible to compare actual measured load distributions with the load distributions calculated by various means. The measured responses were compared with AASHTO values and values calculated by a method developed by the authors in 1987. The latter, an extension of the Guyon-Massonnet method, was found to produce less conservative and more accurate results than the AASHTO method. Full-speed and crawl test data were analyzed in order to calculate dynamic impact factors for this structure. These values were also compared with the AASHTO design impact factors.

The Holston River Bridge carries Interstate-40 over the Holston River just east of Knoxville, Tennessee. The bridge supports six lanes of traffic, three in each direction. Four continuous steel girders support a concrete deck 7½ in. (19 cm) thick that acts compositely with the girders. The roadway shoulder is supported by cantilever extensions that frame into the web of the exterior girders (Figure 1). The girders vary in depth throughout the length of the bridge but are identical at any given cross section. The bridge is 363.8 m (1,193 ft) in total length and consists of seven spans ranging in length from 41.2 m (135 ft) to 73.2 m (240 ft) (Figure 2). Within the single 73.2-m span, the girders are connected laterally by cross trusses at 6.7 m (22 ft) on center (Figure 3, *top*). In all other spans, floor beams run between the girders (Figure 3, *bottom*). Both the trusses and floor beams support two wide flange sections each that serve as stringers for the bridge deck.

In January 1992, the Tennessee Department of Transportation discovered a fatigue failure in the outside girder on the eastbound lane. The fracture was located near the one-third point of the 73.2-m span between Piers 1 and 2 directly over the main channel of the river (Figure 4). The fracture extended almost the entire depth of the member. A large gap was present at the bottom flange of Girder 4. The two outside lanes of the bridge were immediately closed to traffic on each side, and measures were taken to repair the damaged girder. A retrofit of the cantilever-to-girder-web connection was also implemented that was intended to eliminate the out-of-plane distortion of the girder web, which had initiated the failure. In January 1993, a research project was begun by the University of Tennessee Transportation Center to investigate the Holston River Bridge fatigue failure. This project had four basic objectives: (a) determine the effectiveness of the retrofit repairs, (b) estimate the portion of the bridge fatigue life expended at the time of failure, (c) estimate the remaining life of the bridge on the basis of current and estimated future use and identify controlling fatigue detail locations, and (d) study critical details of the bridge structure for potential fatigue problems resulting from dynamic response of the structure. In order to accomplish these objectives, extensive field testing was required. First, careful inspection of the bridge plans and the bridge itself revealed the location of several critical points. Members at these locations were then instrumented with strain gauges. Strain gauge data were collected under both normal traffic and controlled loads. The information from these gauges was used to determine the response of the structure under these loads. Details of this investigation and results of the fatigue study will be reported in other papers. The focus of this paper is limited to a consideration of (a) dynamic load factor and (b) lateral distribution of loads.

This paper provides a summary of the controlled load tests performed on the Holston River Bridge. The structural behavior of the bridge when subjected to a controlled load was examined in detail. Lateral distribution of these loads to the four longitudinal girders was examined, and the measured distributions were compared with distributions obtained by analytical methods (*1*) and those recommended by AASHTO. The results of both the dynamic and static controlled load tests were analyzed and the data were compared in order to determine a dynamic impact factor for the structure. These values were also compared with AASHTO values.

REVIEW OF LITERATURE

Dynamic Impact Factors

Data including dynamic impacts and girder distributions were collected and incorporated into a system to evaluate bridge safety by Ghosn et al. (*2*). Dynamic impact factors calculated from these data were compared with AASHTO values; the AASHTO values were found to be conservative.

Dynamic impact factors were considered in NCHRP Report 301 (*3*). Impact factors taken from a data base of previous studies are given for various sites. It was determined that impact was directly related to roadway roughness. Instructions are provided in the report for selecting categories for a given roadway.

J. H. Deatherage, D. W. Goodpasture, and E. G. Burdette, Department of Civil Engineering, University of Tennessee, Knoxville, Tenn. 37996-2010. M. D. Sanders, Forcum-Lannom, Dyersburg, Tenn. 38025-0768.

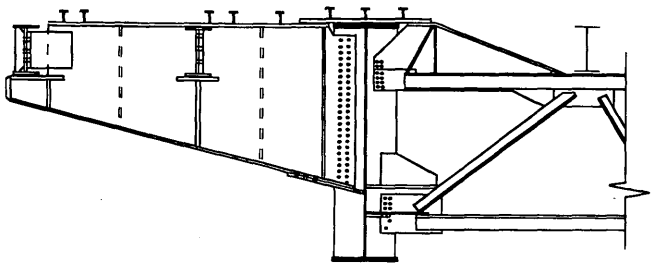

FIGURE 1 Cantilever-to-girder connection.

The effect of truck weight on the dynamic impact factor was examined by Nowak (*4*). It was found that as truck weight increased, the dynamic impact factor decreased.

Lateral Load Distribution

Present AASHTO distribution factors have been found to be conservative by many researchers (*5–7*). This research has encompassed different means, including analytical methods, computer models, scale models, and actual field measurements. The work by Sanders and Elleby referenced Guyon and Massonnet extensively in developing the current AASHTO load distribution factors. Deatherage (*5*) extended the Guyon-Massonnet theory to develop a series of influence coefficients that more accurately represent the effects of a load applied laterally on the cross section of a beam-slab bridge. In Deatherage's work, a torsional parameter, α, and a flexural stiffness parameter, Θ, are used to determine the appropriate influence coefficients to be used with a particular structure.

The effect of different variables on lateral distribution was examined by Hays et al. (*6*) through the use of a computer program, Structural Analysis for Load Distribution (SALOD). AASHTO factors were found to produce conservative results when compared with the results from SALOD.

An experimental test program was used to evaluate the behavior of a 4/10-scale model of a two-span continuous plate girder bridge (*7*). Distribution factors computed using AASHTO procedures were found to be quite conservative for the interior girder and less so for the exterior girders.

Field data were collected using strain gauges and weigh-in-motion (WIM) equipment. These data were used to calculate lateral distribution factors and dynamic impact factors. When these values were compared with AASHTO values, the AASHTO values were again found to produce conservative results.

Nowak et al. (*1*) also used strain gauges and WIM equipment to evaluate a structure's response to traffic. The structure was a multispan bridge supported by four steel plate girders. In addition to evaluation of the bridge details with respect to fatigue damage, measured girder moment distribution factors are presented for the structure.

CONTROLLED LOAD TESTS

On August 5, 1993, control tests were performed on the Holston River Bridge using a truck of known weight and axle spacing under controlled traffic conditions. The test vehicle, a tandem-axle dump truck, was provided by the Tennessee Department of Transportation. The total weight of the truck was 341.6 kN (76,760 lb). The weight on the front axle was 67.9 kN (15,260 lb). The two rear axles combined to support 273.7 kN (61,500 lb). The wheel base of the truck was 4.27 m (14 ft 11 in.) from the front to the first rear axle and 5.87 m (19 ft 4 in.) from front to the second rear axle (Figure 5). The width measured 2.36 m (7 ft 9 in.) from outside to outside of the rear tires. The tests were conducted in the early morning hours to minimize the disruption of traffic flow. Tests were begun at 1:00 a.m. and no other traffic was allowed on the bridge when data were being taken. During all test runs an observer from the research team was in the truck to ensure that the driver was in the proper lane and traveling at the proper speed.

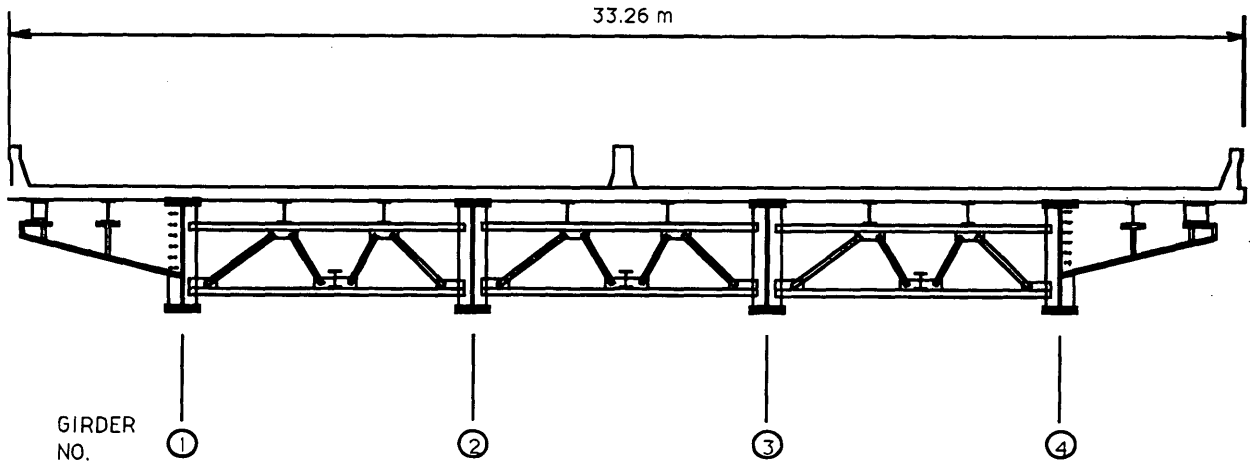

FIGURE 2 Typical cross section.

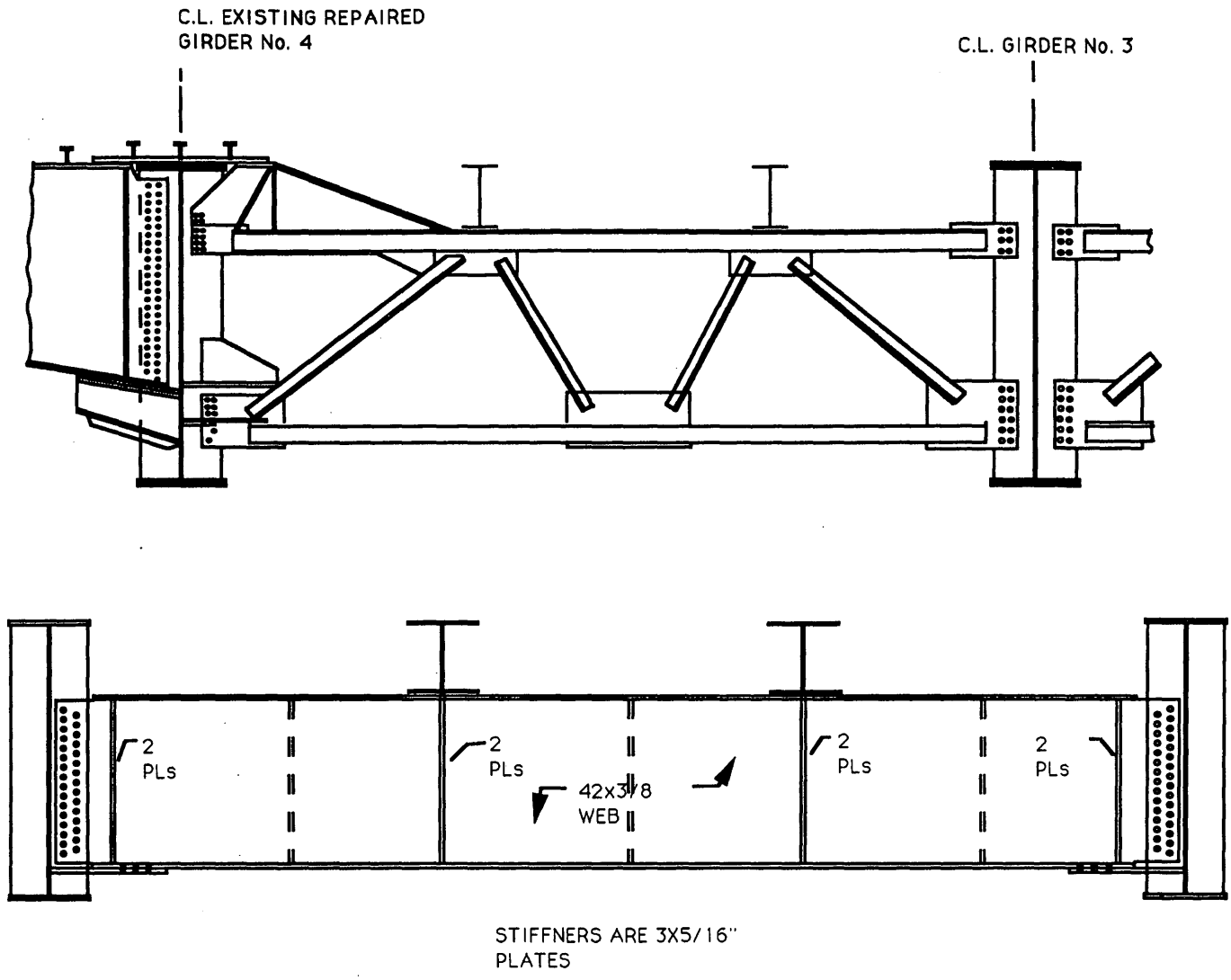

FIGURE 3 *Top*, typical floor truss; *bottom*, typical transverse floor girder.

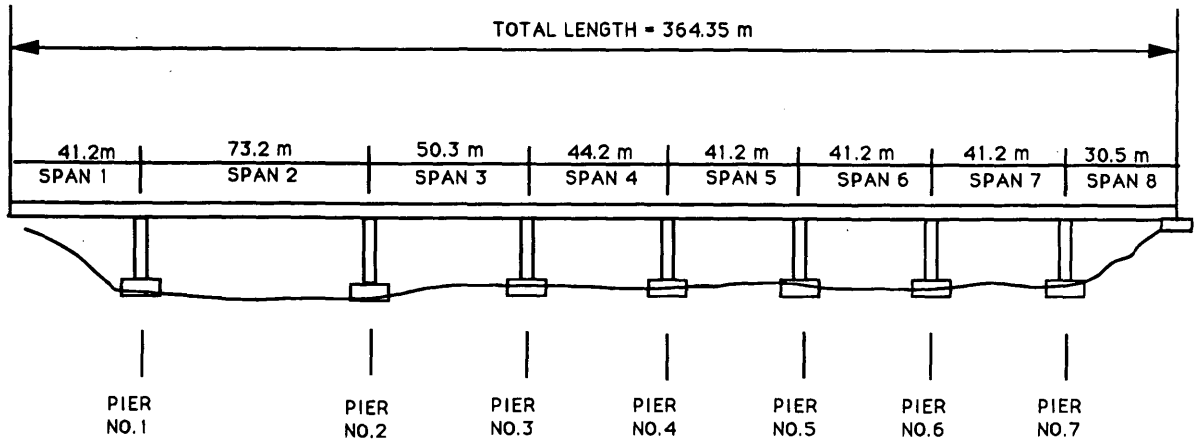

FIGURE 4 Elevation looking north.

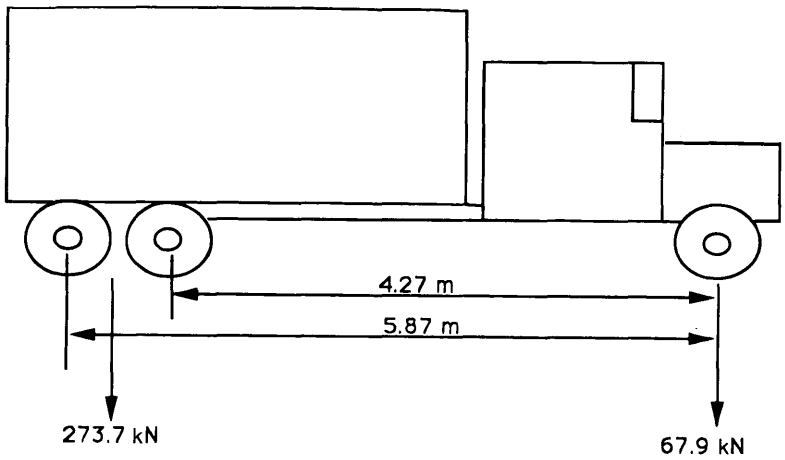

FIGURE 5 Test vehicle for controlled load test.

Tests were conducted at crawl speeds to determine the structure's response to a static load moving along the length of the bridge. A constant speed of 8.05 km/hr (5 mph) was maintained. Data collection for the eastbound crawl tests was begun when the truck reached the west abutment and was stopped when the truck reached the fourth span. All gauge locations were in the first and second spans. The effect of the load on these locations was therefore negligible by the time the truck reached the fourth span. The westbound tests were begun with the truck at approximately the center of the fourth span and ended when it crossed the west abutment. Crawl test data were taken for all six traffic lanes and for both shoulders. Data were also collected when the truck was returning from the end of each run. This allowed two data-collection passes in each lane.

Dynamic tests were also conducted with the truck at speeds ranging from 80.5 km/hr (50 mph) to 104 km/hr (65 mph). The tests with lower speeds were in the eastbound lanes because of the proximity

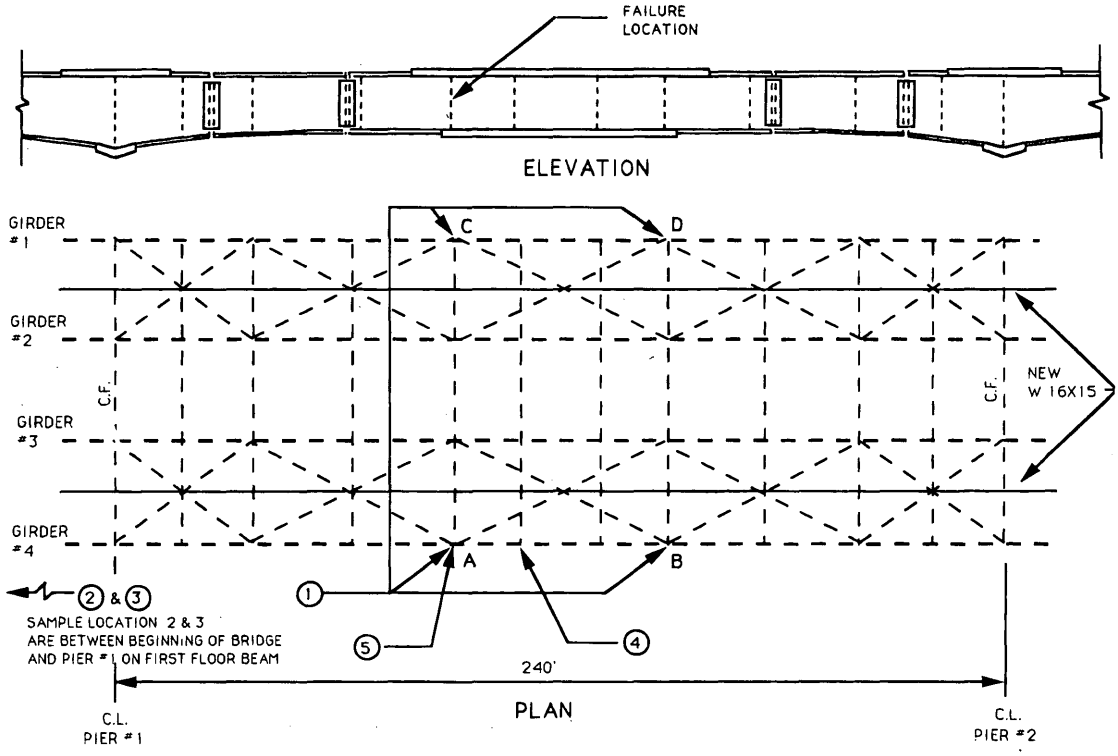

FIGURE 6 Data sample locations.

of the nearest exit west of the bridge. The truck was only able to obtain a speed of around 80.5 km/hr (50 mph) in this relatively short distance. Data were collected for passes with the truck in all six traffic lanes. No dynamic data were taken for the shoulder lanes. The dynamic test data were also collected only when the truck was in the first three spans.

Thirty-one gauges were monitored during these tests. Gauges on the top and bottom flanges of the girders were monitored at locations 1A, 1B, 1C, and 1D (Figure 6). Gauges on the two interior girders at the cross section where the failure occurred were also monitored. Balancing problems prevented obtaining data on the flange of Girder 2. Gauges at the coped ends of the floor girders in Span 1 were also chosen to be monitored. However, only data from the bottom gauge were obtained because of a problem with the top gauge just before the test.

TEST RESULTS

Strains recorded using the MegaDec and the TCS 3000 software were analyzed using an electronic spreadsheet program. The ability to manipulate large amounts of numerical data quickly and easily made the spreadsheet program ideal for analyzing the controlled load test data. To utilize the spreadsheet, data from TCS 3000 had to be converted to a format compatible with the spreadsheet program. This was done by exporting the data into a Data Interchange File (DIF) within the TCS 3000 program. Once converted, the file was transferred to the spreadsheet program where manipulation of the data was possible.

Strain gauge readings were taken at a rate of 60 Hz. Although the spreadsheet was capable of handling any of the test files transferred from TCS 3000, the files were quite large and required a great deal of memory. A lower sample rate would have adequately reflected the structure's behavior during the controlled load tests. Once the data were transferred to the spreadsheet, they were reduced to reflect a sample rate of 10 Hz by creating a macro within the spreadsheet that automatically deleted the appropriate data from each test file.

The spreadsheet program also allowed the creation of plots for any given gauge in any given test (Figure 7). Data from each test were reduced and analyzed. Maximum stresses at gauge locations of interest were determined for each of the test runs. Tables 1 and 2

TABLE 1 Maximum Main Girder Stresses for Crawl Tests (MPa)

		EAST BOUND			
GIRDER #		SHOULDER	RIGHT LANE	MIDDLE LANE	LEFT LANE
1	POS	0.71	1.42	1.19	1.42
	NEG	-2.84	-1.18	-0.48	-1.65
	RANGE	3.55	2.60	1.65	3.07
3	POS	4.26	6.16	9.47	9.94
	NEG	-3.31	-2.13	-2.13	-2.84
	RANGE	7.57	8.29	11.60	12.78
4	POS	17.52	170.51	10.65	5.45
	NEG	-5.44	-37.85	-3.32	-3.32
	RANGE	22.96	20.84	13.97	8.76

		WEST BOUND			
GIRDER #		SHOULDER	RIGHT LANE	MIDDLE LANE	LEFT LANE
1	POS	14.44	13.73	9.23	5.21
	NEG	-4.26	-3.32	-2.84	-2.36
	RANGE	18.71	17.05	12.07	7.58
3	POS	1.65	2.36	3.79	5.45
	NEG	-1.18	-2.13	-1.42	-1.42
	RANGE	2.84	8.29	5.21	6.87
4	POS	1.42	0.94	1.19	2.84
	NEG	-2.84	-1.65	-0.71	-0.94
	RANGE	4.26	2.60	1.90	3.79

Divide stresses by 6895×10^{-3} to convert to psi.

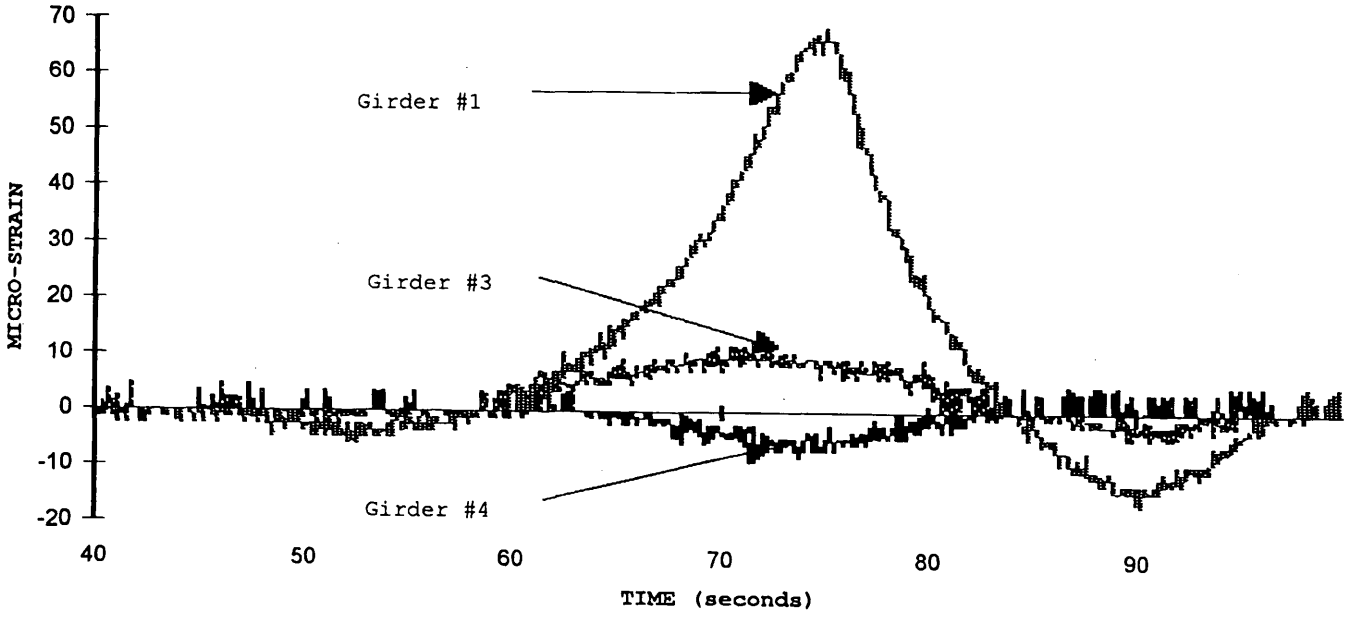

FIGURE 7 Typical gauge outputs for controlled load crawl test data, westbound right lane.

TABLE 2 Maximum Measured Main Girder Stresses for Dynamic Tests (MPa)

GIRDER #		EAST BOUND			
		SHOULDER	RIGHT LANE	MIDDLE LANE	LEFT LANE
1	POS	N/A	2.61	1.19	2.14
	NEG	N/A	-1.19	-1.19	-0.71
	RANGE	N/A	3.79	2.36	2.84
3	POS	N/A	6.38	10.18	13.25
	NEG	N/A	-2.85	-2.36	-1.65
	RANGE	N/A	9.23	12.55	14.92
4	POS	N/A	16.81	10.65	6.86
	NEG	N/A	-5.21	-4.10	-2.60
	RANGE	N/A	22.02	14.68	9.47

GIRDER #		WEST BOUND			
		SHOULDER	RIGHT LANE	MIDDLE LANE	LEFT LANE
1	POS	N/A	14.92	8.76	5.68
	NEG	N/A	-3.07	-4.02	-2.36
	RANGE	N/A	17.99	12.78	8.05
3	POS	N/A	1.35	3.075	4.97
	NEG	N/A	-1.59	-1.42	-1.42
	RANGE	N/A	2.95	4.49	6.39
4	POS	N/A	1.65	0.94	2.36
	NEG	N/A	-1.89	-1.18	-1.65
	RANGE	N/A	3.55	2.13	4.02

Divide stresses by 6895×10^{-3} to convert to psi.

show the maximum stresses at the main girder bottom flange for the crawl tests and the dynamic tests, respectively, Figure 8 shows a typical plot of static versus dynamic test data. Data from two other areas of interest were also examined. These two areas were believed to be locations of high stress and susceptible to fatigue damage. Table 3 shows maximum stress ranges at the web gap on Girder 1. The values for the test runs with the truck in the westbound lanes are given. Test runs with the truck in the eastbound lanes had little effect on this location. Table 4 shows the maximum stress ranges for the floor beam in the area of the termination of its bottom flange near its connection to the interior girder.

TABLE 3 Maximum Stress Ranges at Web Gap on Girder 1 (MPa)

TRUCK POSITION	MAXIMUM STRESS RANGE (MPa)	
	STATIC	DYNAMIC
WEST BOUND LEFT LANE	14.44	16.09
WEST BOUND MIDDLE LANE	21.54	23.67
WEST BOUND RIGHT LANE	26.51	28.64

Divide stresses by 6895 x 10^{-3} to convert to psi.

ANALYSIS OF DATA

It has been shown by several other researchers that the approximations commonly used for design to predict stresses in members produce conservative results (*1,6,7*). The Holston River Bridge project provided an excellent opportunity to measure the response of an actual structure to applied loads. Data collected during the controlled load tests provide a means of evaluating the accuracy of assumptions and simplifications made during the design of this and other bridges. The data were analyzed and compared with results obtained using analytical methods developed by other researchers (*5*) in an attempt to verify the results of these methods. The actual measured responses were also compared with values obtained using AASHTO values.

Deatherage (*5*) attempted to provide engineers with a simplified means of evaluating load distributions for beam-slab bridges. He extended the Guyon-Massonnet theory and developed a series of influence coefficients that can be used to predict the effect of a load applied laterally at any point on the cross section of a bridge. The values of these influence coefficients depend on a flexural parameter, Θ, and torsional parameter, α, which are specific to the particular structure being evaluated. Curves representing influence coefficients versus the relative lateral location of loads for the Holston River Bridge were developed (Figures 9 and 10). From these curves, distribution coefficients for interior and exterior girders for test trucks in all six lanes were calculated.

AASHTO uses a distribution factor based on the girder spacing divided by a constant for a particular type of structure. An AASHTO distribution coefficient obtained by dividing the girder spacing by 5.5 was calculated.

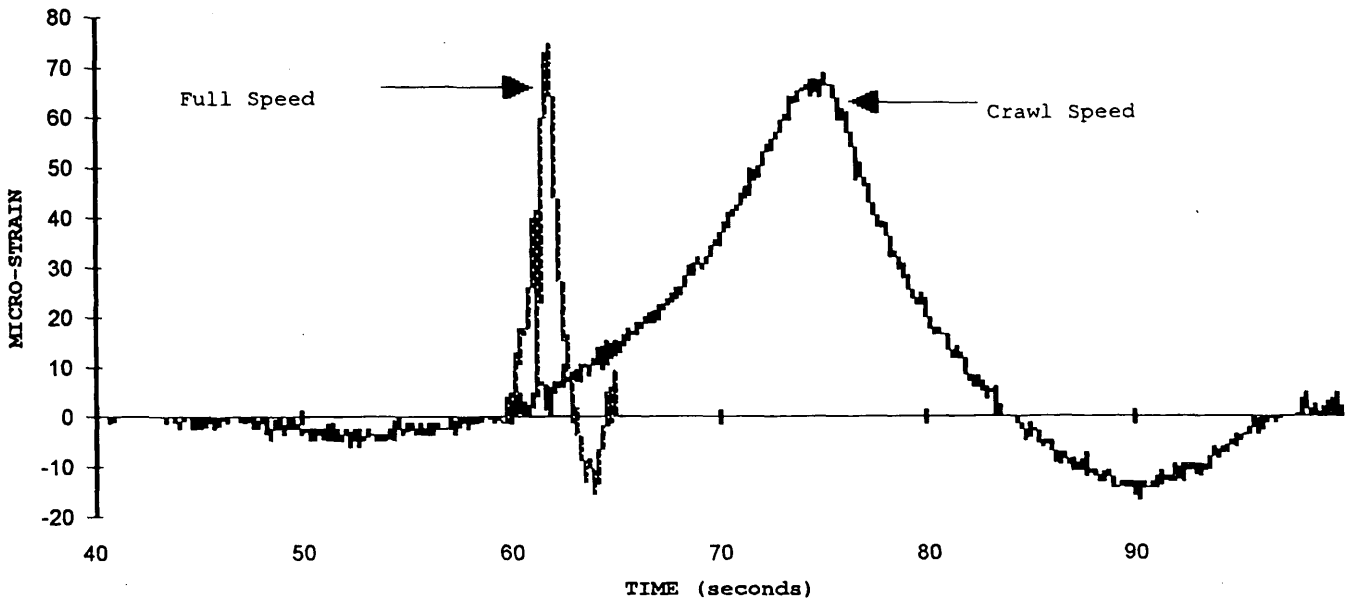

FIGURE 8 Typical gauge outputs for controlled load crawl and fullspeed test data, westbound right lane.

TABLE 4 Maximum Stress Ranges at Floor Beam Bottom Flange Termination (MPa)

TEST RUN	STRESS RANGE (MPa)	
	STATIC	DYNAMIC
EAST BOUND SHOULDER	15.63	N/A
EAST BOUND RIGHT LANE	12.78	13.96
EAST BOUND MIDDLE LANE	7.81	12.54
EAST BOUND LEFT LANE	21.31	28.41
WEST BOUND LEFT LANE	5.21	10.18
WEST BOUND MIDDLE LANE	6.63	7.81
WEST BOUND RIGHT LANE	10.89	12.54
WEST BOUND SHOULDER	13.25	N/A

Divide stresses by 6895 x 10^{-3} to convert to psi.

By superimposing measured maximum stresses for each pass of the test truck, maximum stresses equivalent to those that would be produced with a truck in all six lanes could be obtained for each girder. These stresses were used to determine an actual distribution factor, which was then compared with both calculated distribution factors.

Computer models for exterior and interior girders were developed using GTSTRUDL. With the aid of these models and the calculated distribution factors, moments for each girder were determined at the bottom flange strain gauge locations. The stresses for the bottom flange of each girder were then calculated using the section properties at strain gauge locations. These stresses were compared with the actual measured stresses at the bottom flanges of the main girders.

Table 5 summarizes the distribution factors and stresses from both methods and actual measurements.

Another important variable in determining design forces in bridge members is the dynamic impact factor. Other researchers have found that the AASHTO allowance for dynamic impact is usually higher than that measured during tests (*1*). AASHTO uses the value

$$I = 50/L + 125)$$

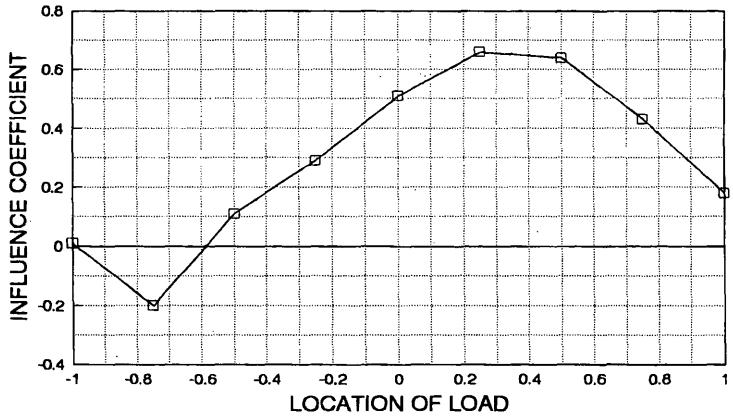

FIGURE 9 Influence coefficients for interior girder at 0.33 (α = 0.132; θ = 1.06).

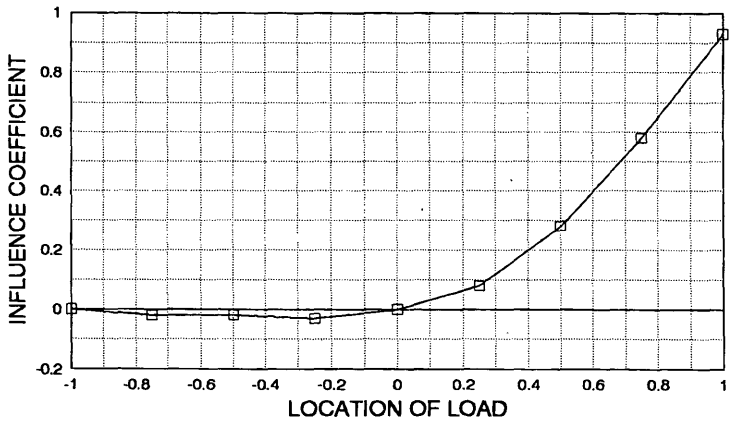

FIGURE 10 Influence coefficients for exterior girder at 1.0 (α = 0.132; θ = 1.06).

TABLE 5 Calculated and Measured Maximum Stresses (MPa)

GIRDER NUMBER	AASHTO		CALCULATED		MEASURED	
	DISTRIBUTION FACTOR	MAX STRESS MPa	DISTRIBUTION FACTOR	MAX STRESS MPa	DISTRIBUTION FACTOR	MAX STRESS MPa
3(interior)**	4.72	79.29	3.38	56.67	2.28	37.16
1(exterior)	4.72	79.29	2.36	39.57	1.92	32.19
4(exterior)	4.72	79.29	2.36	39.57	2.27	38.12

**Stresses were not measured for interior girder #2
Divide stresses by 6895 x 10^{-3} to convert to psi.

TABLE 6 Dynamic Impact Factor for Girders

TEST RUN	GIRDER #	MAX STRESS RANGE		MEASURED IMPACT FACTOR
		STATIC	DYNAMIC	
RIGHT	1	2.60	3.78	N/A*
LANE	3	8.28	9.23	1.11
E. BOUND	4	20.83	22.02	1.06
MIDDLE	1	1.65	2.36	N/A*
LANE	3	11.60	12.54	1.08
E. BOUND	4	13.96	14.67	1.05
LEFT	1	3.07	2.84	N/A*
LANE	3	12.78	14.92	1.17
E. BOUND	4	8.76	9.47	1.08
RIGHT	1	17.05	17.99	1.06
LANE	3	3.31	2.95	N/A*
W. BOUND	4	2.60	3.55	N/A*
MIDDLE	1	12.07	12.79	1.06
LANE	3	5.21	4.49	N/A*
W. BOUND	4	1.89	2.13	N/A*
LEFT	1	7.57	8.05	1.06
LANE	3	6.86	6.39	N/A*
W. BOUND	4	3.78	4.02	N/A*

Divide stresses by 6895 x 10^{-3} to convert to psi.

for the increase in live load due to dynamic impact. This equation takes the span length as its only variable. However, research has shown that the dynamic impact factor is directly controlled by road surface roughness (*2,4*).

During the controlled load tests on the Holston River Bridge, data were taken for both crawl and full-speed tests. Comparing the maximum stresses in the two sets of tests allowed the determination of an actual impact factor. Impact factors were calculated for three locations on the bridge, including the bottom flange of the main girders in Span 2, the web gap on Girder 1 in Span 2, and the floor beam in Span 1. The test runs that produced maximum stresses below 6.89 MPa (1,000 psi) were not included in the calculations because of the more pronounced effect of outside interference on these readings. These factors were then compared to the AASHTO value of $50/(L + 125)$. Tables 6, 7, and 8 show the dynamic impact values for each location along with the AASHTO values.

TABLE 7 Dynamic Impact Factors for Web Gap on Girder 1

TEST RUN	MAX STRESS RANGE		MEASURED IMPACT FACTOR
	STATIC	DYNAMIC	
WEST BOUND LEFT LANE	14.44	16.09	1.11
WEST BOUND MIDDLE LANE	21.54	23.67	1.10
WEST BOUND RIGHT LANE	26.51	28.64	1.08

Divide stresses by 6895 x 10^{-3} to convert to psi.

TABLE 8 Dynamic Impact Factors for Floor Beam

TEST RUN	MAX STRESS RANGE		MEASURED IMPACT FACTOR
	STATIC	DYNAMIC	
EAST BOUND SHOULDER	15.63	N/A	N/A
EAST BOUND RIGHT LANE	12.78	13.96	1.09
EAST BOUND MIDDLE LANE	7.81	12.54	1.61
EAST BOUND LEFT LANE	21.31	28.41	1.33
WEST BOUND LEFT LANE	5.21	10.18	N/A
WEST BOUND MIDDLE LANE	6.63	7.81	1.18
WEST BOUND RIGHT LANE	1580	1820	1.15
WEST BOUND SHOULDER	1923	N/A	N/A

Divide stresses by 6895 x 10^{-3} to convert to psi.

CONCLUSIONS

AASHTO provides a simple method for determining the lateral distribution of loads on a particular girder. This method, however, has been shown to produce very conservative results in the case of the Holston River Bridge as well as for others (*5–7*). The AASHTO factors led to the calculation of stresses that were in excess of two times the actual measured stresses for both interior and exterior main girders. Although sophisticated computer modeling techniques can potentially provide much more accurate results, the time involved and level of expertise required may outweigh the benefits of a more precise solution. The need for a methodology that quickly and accurately predicts the portion of applied load carried by a single member is evident. Even when a more sophisticated computer model is to be used, a method accurate enough to verify its results is useful. Deatherage (*5*) attempted to provide such a method; his method accounts for both bending and torsional stiffness in laterally distributing the loads. When applied to the Holston River Bridge, this method produced results that, although still conservative, were less conservative than the AASHTO values for both the interior and exterior girders. The method proved to be extremely accurate for the exterior girders and less so for the interior. However, this method does provide a simple and quick procedure for determining the appropriate amount of applied loads to assign to longitudinal members.

The dynamic impact factor used by AASHTO has been shown by several researchers to be higher than that actually measured in some cases (*4*). The AASHTO equation for the dynamic impact factor takes only one variable into consideration, span length. A review of the recent research on the effect of variables on the dynamic impact factor shows that roadway roughness rather than span length is the controlling factor.

The values measured on the Holston River Bridge varied depending on the location being considered. The measured impact factors for the main girders in Span 2 compared relatively well with the AASHTO value (*8,3*). Although one test run produced a value above the AASHTO value, the measured values were consistently lower than calculated. The measured values at the floor beam in Span 1, however, do not compare well with the AASHTO value (*8,1*). The AASHTO value to be used for this location was calculated using the span length of the main girders in Span 1 41.2 m (135 ft), as is believed to be normal practice. There was evidence that this value when applied to the floor beams is unconservative.

REFERENCES

1. Nowak, A. S., H. Nassif, and K. H. Frank. Fatigue Load Spectra for Steel Girder Bridge. In *Transportation Research Record 1393*, TRB, National Research Council, Washington, D.C., 1993.
2. Ghosn, M., F. Moses, and J. Gobieski. Evaluation of Steel Bridges Using In-Service Testing. In *Transportation Research Record 1072*, TRB National Research Council, Washington, D.C., 1986.
3. Moses, F. and D. Verma. *NCHRP Report 301: Load Capacity Evaluation of Existing Bridges*. TRB, National Research Council Washington, D.C., 1987.
4. Nowak, A. S., Y. K. Hong, and E. S. Hwang. Modeling Live Load and Dynamic Load for Bridges. In *Transportation Research Record 1290*, TRB, National Research Council, Washington, D.C., 1991.
5. Deatherage, J. H. *Investigation of Variables Affecting Beam-Slab Bridge Load Capacity*. Ph.D. dissertation. University of Tennessee at Knoxville, June 1987.
6. Hays, C. O., L. M. Sessions, and A. J. Berry. Further Studies on Lateral Load Distribution Using a Finite Element Method. In *Transportation Research Record 1072*, TRB, National Research Council, Washington, D.C., 1986.
7. Moore, M., K. A. Strand, M. A. Grubb, and L. R. Cayes. Wheel-Load Distribution Results from AISI-FHWA Model Bridge Study. In *Transportation Research Record 1275*, TRB, National Research Council, Washington, D.C., 1990.
8. *Standard Specifications for Highway Bridges*, 13th ed. American Association of State Highway and Transportation Officials, Washington, D.C., 1983.

Publication of this paper sponsored by Committee on Dynamics and Field Testing of Bridges.